Biochemical and Biophysical Research Communications 450 (2014) 189–194

Contents lists available at ScienceDirect

Biochemical and Biophysical Research Communications

journal homepage: www.elsevier.com/locate/ybbrc

Identification of lysosomotropic compounds based on the distribution and size of lysosomes

Incheol Seo [a], Bijay Kumar Jha [a], Jeong-Geun Lim [b], Seong-Il Suh [a], Min-Ho Suh [a], Won-Ki Baek [a,c,*]

[a] Department of Microbiology, School of Medicine, Keimyung University, Daegu, Republic of Korea
[b] Department of Neurology, School of Medicine, Keimyung University, Daegu, Republic of Korea
[c] Institute for Cancer Research, School of Medicine, Keimyung University, Daegu, Republic of Korea

ARTICLE INFO

Article history:
Received 9 May 2014
Available online 27 May 2014

Keywords:
Lysosomotropism
High-contents screening
Lysosome size
Lysosome distribution

ABSTRACT

Lysosomal accumulation of drugs with their specific physicochemical properties is of key importance to drug distribution in the body. Several attempts have been made to treat various human diseases by employing the accumulation of lysosomal drugs, and many methods to identify lysosomal accumulation of drugs have been proposed. Among those, the use of high-content screening has increased tremendously because of improved efficiency and accuracy as well as the development of automatic image acquisition and analytical techniques. Conventional methods to identify lysosomal accumulation of drugs by evaluating changes in the lysosomal area are unable to maximize the advantages of phenotypic high-content screening. Lysosomal distribution and the size of lysosomes are affected by lysosomal accumulating drugs. Therefore, we present image acquisition conditions and analytical methods to utilize lysosomal distribution and size as parameters for identifying lysosomal accumulating drugs. These two parameters will help to improve the reliability of the screening methods for identifying lysosomal accumulation of drugs by maximizing usage of information from image-based screening.

1. Introduction

Lysosomes are small intracellular organelles essential for the breakdown of cellular debris, waste material, and engulfed microbes. There are more than 50 lysosomal enzymes that can breakdown lipids, phospholipids, glycolipids, proteins, nucleic acids and sugars [1,2]. These enzymes remain active in the acidic environment of the lysosome (pH 4.5–5.0) [3], which is maintained through proton pumps (vacuolar H^+-ATPase) on the lysosomal membrane [4]. This acidic environment allows some drugs to accumulate within the lysosome. These drugs called lysosomotropic agents have a lipophilic and basic moiety. Their high lipophilicity ($\log P > 1$) allows them to pass through the cell and lysosome membranes by diffusion [5]. After diffusing into the lysosome, these compounds are protonated by the acidic environment due to their high acid dissociation constants (pKa > 7) and are sequestered within the lysosome because positively charged compounds are impermeable to the lysosomal membrane [6]. This phenomenon is referred as lysosomotropism. As a result, lysosomal pH becomes more alkaline than optimal by protonation of these compounds [7]. Lysosomotropism of drugs should be considered a possible harmful factor because of the cytotoxicity and non-specific side effects caused by lysosomal accumulation of the drug itself and excessive phospholipids that have been diffused into lysosome combined with the lysosomotropic agent [8].

Various screening methods for identifying lysosomotropic compounds have been suggested [2,9–12]. Among them cell-based methods using fluorescence accumulated specifically within the lysosome are common techniques. In the high-throughput screening (HTS) approach, the accumulation of lysosomotropic compounds is estimated by measuring the intensity of lysosomotropic fluorescence from lysosomal lysates or intact lysosomes. High-content screening (HCS) methods are based on image analysis techniques using two or more fluorescent materials specific to the lysosome, cytoplasm, or nucleus by comparing each fluorescent area to evaluate the lysosomotropic properties of the compounds. Cheminformatic prediction helps to identify lysosomotropism by calculating the lipophilicity (clogP) and pKa of the drug based on quantitative structure–activity relationship models [13]. The HTS method is convenient; however, it requires MTS and LDH assays to detect compound cytotoxicity. Furthermore, to solve the problems caused by the different cytotoxic effects, pKas, and diffusion rates (due to different molecular weights, chemical structures

* Corresponding author. Address: Department of Microbiology, School of Medicine, Keimyung University, 1095 Dalgubeol-daero, Dalseo-Gu, Daegu, Republic of Korea. Fax: +82 53 580 3788.
E-mail address: wonki@dsmc.or.kr (W.-K. Baek).

http://dx.doi.org/10.1016/j.bbrc.2014.05.091
0006-291X/

and lipophilicity.) between compounds, multiple dose and time point drug treatments are required to prepare a concentration response curve to determine lysosomotropism of a drug. This leads to an increased experimental size to obtain reliable results. It is possible to achieve more accurate results using HCS compared to HTS because the HCS method is based on high resolution image analysis. A large number of images can be obtained in a short time and can be analyzed in a high-throughput manner. Nevertheless, image-based HCS cannot achieve satisfactory results because earlier HCS methods only used simple comparisons of the area of fluorescence accumulated in the lysosome with the area of fluorescence specific to the cytoplasm and/or nucleus.

Lysosomes are dynamic organelles and shifting of intracellular localization by alterations in cytoplasmic pH has been reported [14,15]. In a two-dimensional image, lysosomes are observed as perinuclear grape-like aggregates due to increased cytoplasmic pH. Therefore, the ratio between aggregated lysosomes and non-aggregated (free) lysosomes can be used as a marker to detect changes in cytoplasmic pH and lysosomal localization. Additionally, lysosomes become enlarged following treatment with a lysosomotropic compound [16]. In this study, we developed a new analytical method to identify lysosomotropism of drugs based on the intracellular distribution and size of lysosomes, and we compared this new method, which maximizes information usage from image-based HCS, with the conventional method.

2. Materials and methods

All chemicals were obtained from Sigma–Aldrich (St. Louis, MO, USA). The black-walled clear-bottom 96-well plates were purchased from In Vitro Scientific (Sunnyvale, CA, USA).

2.1. Cell culture

The MDA-MB-231 breast cancer cell line was obtained from the Korean Cell Line Bank. Cells were grown at 37 °C in a humidified atmosphere of air containing 5% CO_2 in culture medium containing high-glucose DMEM supplemented with 10% fetal bovine serum, 100 U/ml penicillin, and 100 μg/ml streptomycin.

2.2. Image acquisition

The overall experimental process was similar with the experiment of Nadanaciva et al. [2]. MDA-MB-231 cells were seeded in black-walled clear-bottom 96-well plates at 17,000 cells/100 μl/well in culture medium and incubated for 24 h. The next day, the culture medium was replaced with 100 μl/well of dosing medium containing either the test compounds or 0.5% DMSO. Test compound wells were run in triplicate for every concentration of each drug. The cells were incubated with the test compounds for 2 h in a humidified atmosphere of air containing 5% CO_2 at 37 °C. The cells were rinsed twice with 200 μl PBS to remove the test compounds. A 100 μl aliquot of dosing medium containing acridine orange (AO; final concentration 3 μg/ml) was then added to each well. The cells were incubated for 15 min, and rinsed twice with 200 μl PBS. The remaining PBS was aspirated, and 50 μl PBS was added to each well. Live-cell image acquisition was performed with a Zeiss laser scanning confocal microscope 510 (Oberkochen, Germany) using a 40× objective. Images were obtained with LSM software (Carl Zeiss) at the center of each well. The green (representing cytoplasm) and red (representing lysosomes) fluorescence of the AO were measured on channels 2 and 1 of the microscope, respectively. Detailed settings of image acquisition are described in Supplementary Table 1. Image acquisition was performed batch by batch from the vehicle to the maximum concentration of a well to minimize possible bias that occurred due to the time required for image acquisition.

2.3. Image analysis

Raw data were exported from LSM Image Browser into PNG files without loss of quality, and PNG images were analyzed in the cytoplasm and lysosomes using ImageJ software. The cytoplasmic and lysosomal area recognition method and the image analyzing process are described in Fig. 1. The ImageJ macro commands are described in Supplementary Protocol 1. The area of cytoplasm and lysosomes, their distribution, and the size of the lysosomes were recognized using the ImageJ macro function, which allows processing of a large number of images automatically. Green fluorescence in the image was recognized as the area of the cell. The Triangle threshold method was applied to include all possible green fluorescent signals [17]. The Remove Outlier function in ImageJ was applied to remove background noise from the confocal microscope. IsoData method was applied to set the threshold from a red color image to recognize lysosomal area [18]. As an area recognition error occurred due to low cell viability and loss of red signals which was estimated by lysosomal membrane permeabilization (LMP) in the fluoxetine (FXT) or paroxetine (PXT) treated groups, the red area was recognized using the Intermodes threshold method instead of IsoData [19]. Thus, it is necessary to select the adequate threshold method in a user-defined manner according to image acquisition conditions. Then, these areas recognized as lysosomes were sorted into aggregated and non-aggregated lysosomes depending on the circularity of each recognized lysosomal area using the Analyze Particles function in ImageJ. These aggregated lysosomes did not indicate an actual aggregation of lysosomes but a phenomenon in which lysosomes gather close to the perinuclear area and appear to be aggregated in a two-dimensional image. Thus, we included only lysosomal area which recognized as an almost perfect circle with non-aggregated lysosomes by applying Circularity value for ImageJ macro ranges from 0.9 to 1. Then, the area ratio of aggregated with non-aggregated lysosomes and individual sizes of non-aggregated lysosomes were calculated. Mean and standard deviation values were calculated from all values obtained, and converted into ratios of the vehicle control value.

3. Results

We selected four lysosomotropic and two non-lysosomotropic drugs to confirm that the distribution and the size of lysosomes can be used as indicators of lysosomotropism of a drug (Table 1). We performed preliminary experiments to determine adequate drug treatment time and ideal confocal microscope imaging conditions. Lysosomal accumulation of lysosomotropic fluorescence, AO, increased following treatment of the representative lysosomotropic compound chloroquine (CQ) (Fig. 2). Lysosomotropic compounds can act as photosensitizing agents [20]. The lysosome is also the main site for photodestruction caused by strong light. Therefore, we tried to use low intensity laser for the shortest time to exclude possible experimental error from photodestruction of the lysosome. Photodestruction of lysosomes was observed following repetitive laser exposure of live cells (Fig. 3, Supplementary Video 1 and 2). It was observed as a flash of green fluorescence around the popping lysosome. The red color of the accumulated AO within the lysosome changed to green due to release of AO into the cytoplasm instantaneously after lysosomal membrane permeabilization, which increased the local concentration of AO in the cytoplasm around the destroyed lysosome. This phenomenon is also called "AO flash" [21]. Lysosomal photodestruction was observed

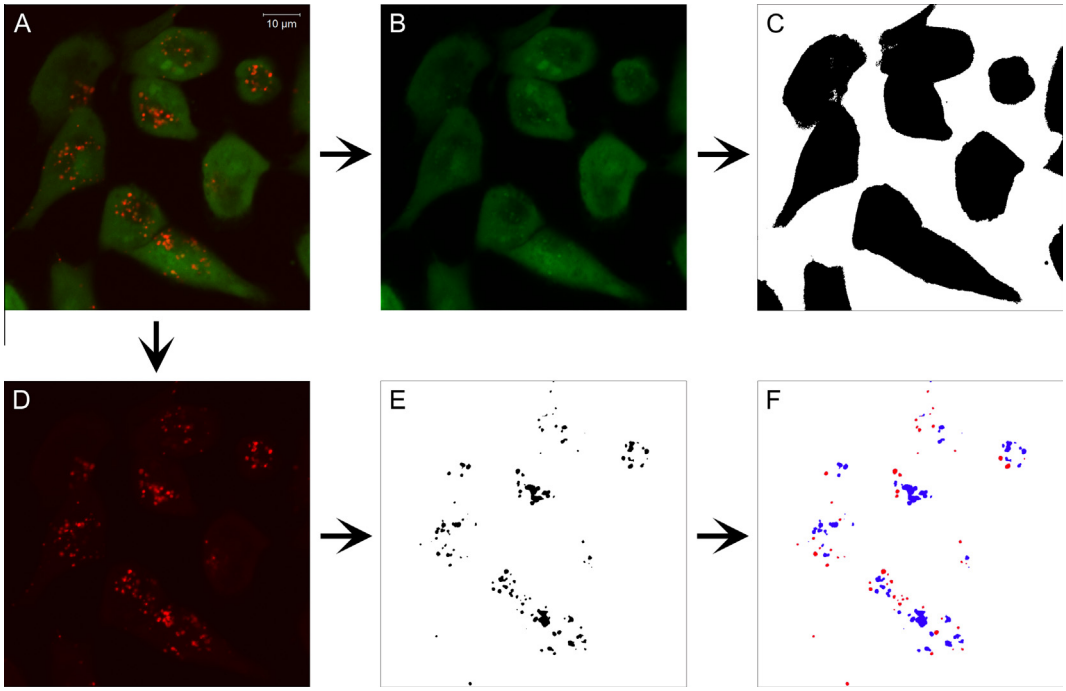

Fig. 1. Raw data were processed for image analysis. (A) The cytoplasm (green) and lysosomes (red) were visualized by acridine orange staining in MDA-MB-231 cells. This is a cropped image from raw data. (B) The cytoplasmic area of green fluorescence was obtained through confocal microscope channel 2. (C) Green fluorescence, which was recognized as the cytoplasm in ImageJ software, is shown in black. Cell viability was determined using the area of the cytoplasm as recognized in C, and designated as black circles (●). (D) Lysosomal area of red fluorescence obtained through confocal microscope channel 1. (E) Red fluorescence, which was recognized as the lysosomes through ImageJ software, is shown in black. The recognized area was normalized by the area of the cytoplasm to calculate conventional parameter, and this conventional parameter was designated by white circles (○). (F) Recognizing lysosomes by classifying aggregated and non-aggregated lysosomes based on their shape. Circular and non-aggregated lysosomes are shown in red. Multiple lysosomes, which look like aggregates, are shown in blue. The distribution of lysosomes was determined based on the degree of lysosomal aggregation by normalizing non-aggregated lysosomes (red) with total lysosomes (recognized area in D), and this was designated by the black squares (■). The size of individual lysosomes was determined by calculating the average size of non-aggregated lysosomes (red), and this is designated as white squares (□). All symbols defined in this figure were designated with same meaning in Figs. 2 and 4 and Supplementary Fig. 1. (For interpretation of the references to color in this figure legend, the reader is referred to the web version of this article.)

Table 1
Fundamental information on the drugs used in this study.

Drug	Molecular species*	AlogP*	Basic pKa*	Lysosomotropism	References
Chloroquine	Base	4.35	10.47	+	[2,24]
Chlorpromazine	Base	4.74	9.41	+	[2,24]
Fluoxetine	Base	4.03	10.05	+	[2,24]
Paroxetine	Base	3.23	9.68	+	[2,25]
Doxycycline	Zwitterion	−0.75	10.84	–	[25,26]
Metformin	Base	−0.74	12.25	–	[26]

* Molecular species and ALogP, Basic pKa values were obtained from chEMBL.

when the cumulative laser exposure time reached about 90 s under our experimental settings (Fig. 3, Supplementary Video 1 and 2, from 8 s). The green color in Supplementary Video 1 was taken while fixing the gain of the detector value and the strength of laser without normalizing the increase in green intensity by time. Intensity of green fluorescence was increased by increasing time of exposure to the excitation light as Jaiswal et al. reported [21]. The green signal in Supplementary Video 2 was normalized by adjusting the detector gain value of channel 2 (green) on the confocal microscope to obtain constant green intensity in every image. Because of these photodestruction of lysosomes, we minimized laser energy for optimal fluorescent excitation. Additionally, the experimental conditions were set to minimize exposure time in a range that we could obtain images with satisfactory resolution for further analysis. The actual image acquisition time and the intensity of laser were set much lower for the further experiments than the preliminary experimental settings because it was necessary to use the laser continuously to obtain high-resolution images. It took 31.46 s to scan 318.4 μm^2 from each well with 1024 × 1024 pixel image. Photodestruction of lysosomes was not observed in the control and low dose lysosomotropic compound-treated group with these settings. However, lysosomal photodestruction was observed with increased green intensity from the cytoplasm (data not shown) in the high concentration of lysosomotropic compound treatment group, which was accompanied by cell death as in the 40 or 80 μM of chlorpromazine (CPZ), FXT, and PXT treatments (Figs. 2 and 3).

Raw data images were acquired under the conditions described above and analyzed by the following process (Fig. 1). Fig. 1A was obtained through two channels of the microscope; the green cytoplasm and red lysosomes were merged and cropped. The green fluorescence of the cytoplasm (Fig. 1B) obtained from channel 1 was converted into an area value of the cell (Fig. 1C). The red fluorescence of the lysosomes obtained from channel 2 (Fig. 1D) was converted into total lysosomal area (Fig. 1E), and divided into the non-aggregated area with the circular shaped lysosomes (Fig. 1F,

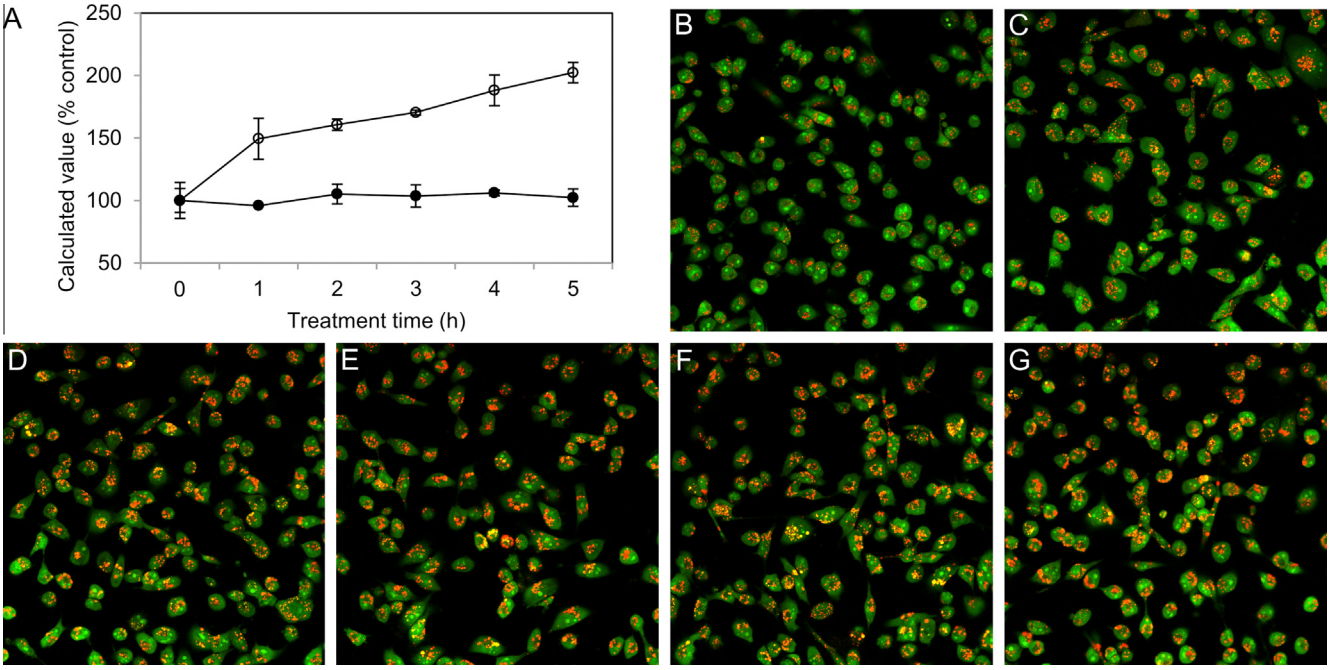

Fig. 2. (A) Changes in the lysosomal area with 20 μM CQ treatment over time through image analysis obtained from confocal microscopy. (○) Changes in lysosomal area normalized by cytoplasm area. (●) Evaluation of cell viability based on the changes in total cytoplasmic area. (B) Immediate after treatment with CQ. (C–F) 1–5 h treatment with CQ respectively. Values represent mean ± standard deviation. CQ; chloroquine.

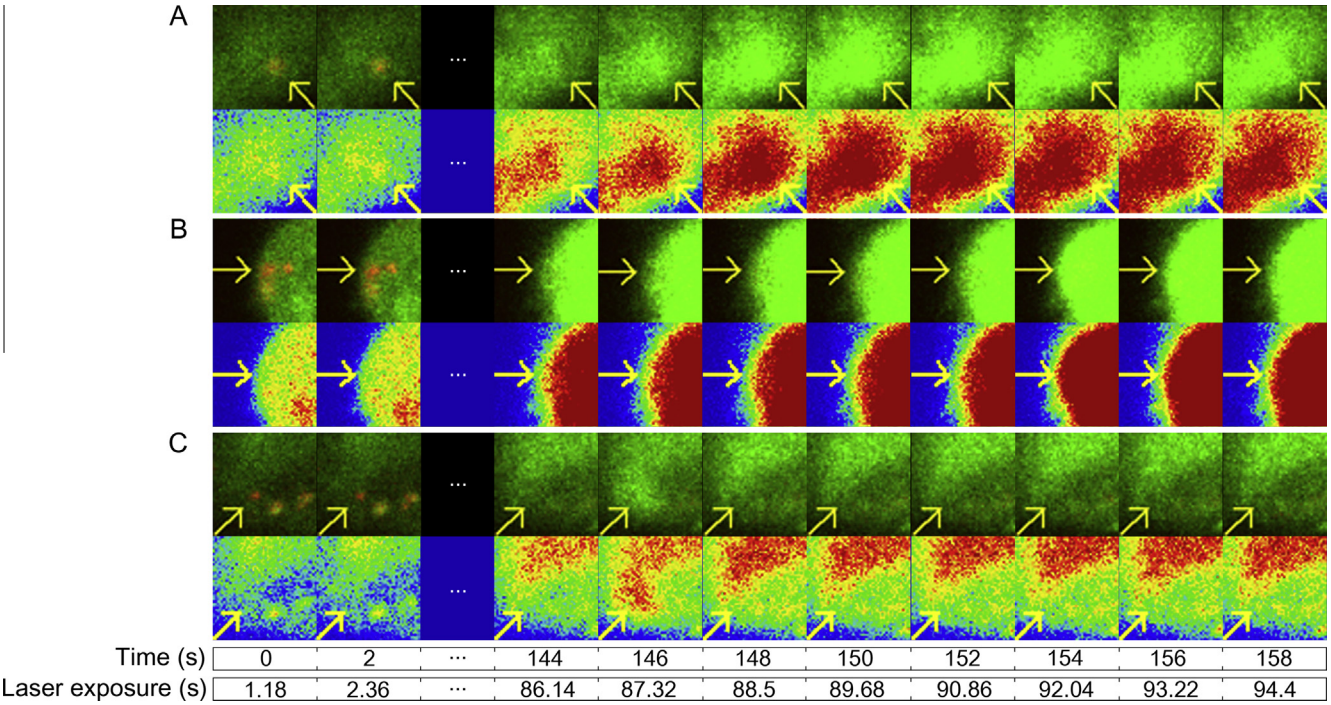

Fig. 3. These images were cropped from Supplementary Video 1. Rainbow overlay was applied for visualizing green fluorescence intensity (second row from A–C). (A and C) Lysosomal photodestruction was observed from laser exposure time reaches 87.32 s. (B) AO flash was observed when laser exposure time reaches 92.04 s.

red) and aggregated lysosomes (Fig. 1F, blue). Each area recognized in Fig. 1C, E, and F was digitized and each parameter was calculated according to Figs. 2 and 4 and Supplementary Fig. 1.

Images from four lysosomotropic compounds and two non-lysosomotropic compounds were analyzed according to the conventional method by comparing the ratio of the total lysosomal area to the total cytoplasmic area for identifying lysosomotropism and to confirm reproducibility of the conventional screening method under the experimental settings described above (Supplementary Fig. 1). An increase in the lysosomal area was observed in the CQ treated group in a dose-dependent manner (Supplementary Fig. 1A, white circles). No change in cell viability was detected up to 80 μM CQ (Supplementary Fig. 1A, black circles). The CPZ treated group also showed an increase in the ratio of lysosomes to cytoplasm (Supplementary Fig. 1B, white circles). A decrease in cell viability was observed beginning at 40 μM. Significant cell death at

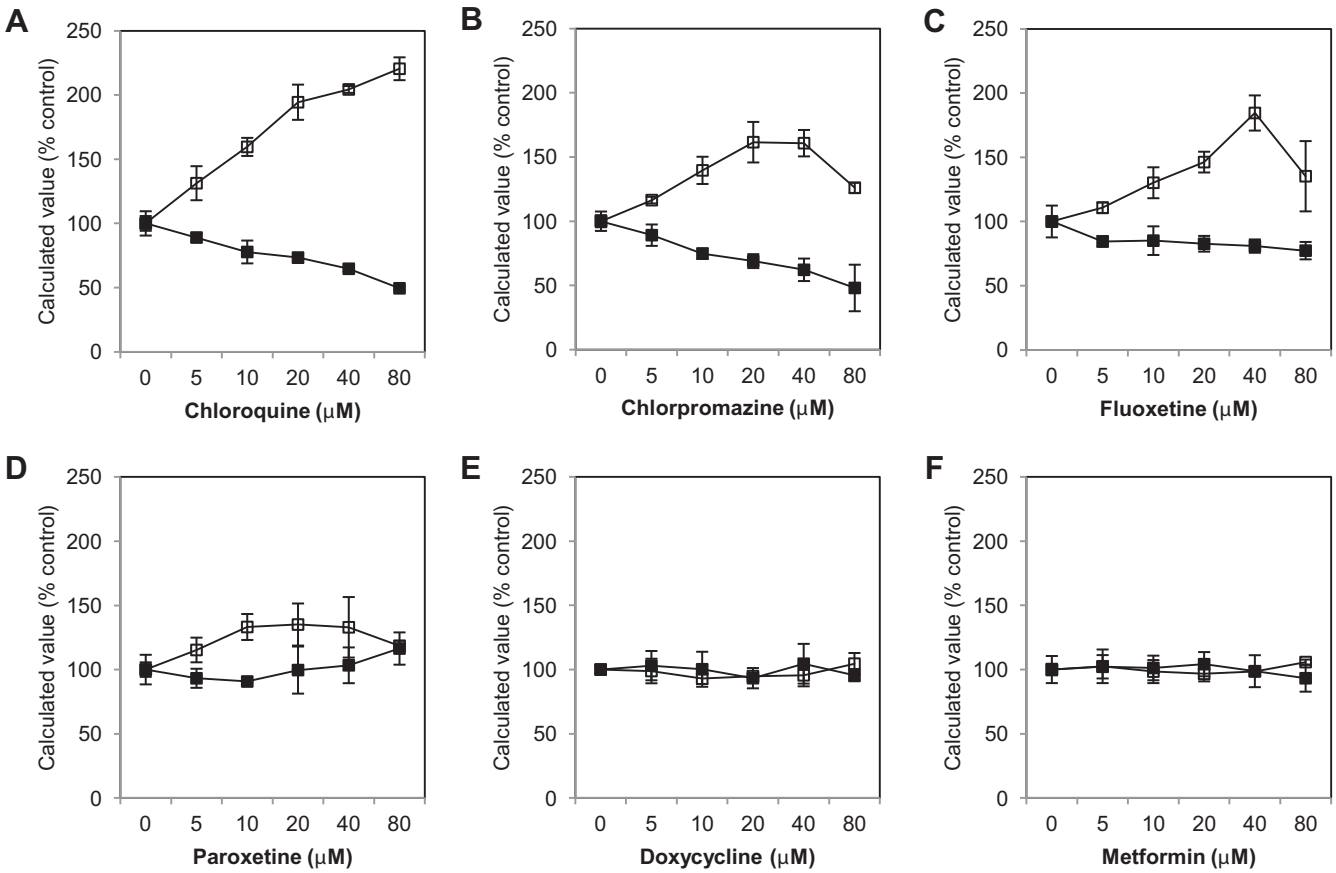

Fig. 4. Identification of the lysosomotropic compounds using new parameters that evaluate the distribution and size of the lysosomes. (■) The ratio of non-aggregated lysosomal area to total lysosomal area. (□) Average size of non-aggregated lysosomes. (A–D) Lysosomotropic compounds. (E and F) Non-lysosomotropic compounds. Values represent mean ± standard deviation of the percentage values relative to the control group ($n = 3$).

80 μM made it difficult to trust the results of increased lysosomal area (Supplementary Fig. 1B). Each group treated with FXT and PXT at up to 20 μM showed an increase in lysosomal area; however, the ratio of lysosomal area decreased due to reduced cell viability beginning at 40 μM (Supplementary Fig. 1C and D) Treatment with doxycycline (DOX), a non-lysosomotropic compound, did not significantly change lysosomal area or cell viability (Supplementary Fig. 1E). The change in the ratio of lysosomal area was not observed in the other non-lysosomotropic compound, metformin (MET), and the cell survival rate decreased slightly beginning at 40 μM (Supplementary Fig. 1F). We confirmed that this conventional analytical method can be used to identify lysosomotropic compounds by comparing the area of the lysosome and the cytoplasm unless cell viability has decreased significantly.

The raw data images used in the analysis of Supplementary Fig. 1 were reanalyzed to verify the possibility of distinguishing lysosomotropic compounds using the distribution and size of lysosomes (Fig. 4). First, the ratio of the total area of non-aggregated lysosomes compared to the area of total lysosomes decreased gradually in a CQ dose-dependent manner (Fig. 4A, black squares). Therefore, we confirmed that lysosomes were aggregated dose dependently by the CQ treatment, and this method correctly recognizes changes in lysosome localization. Second, the average size of non-aggregated lysosomes increased in a CQ dependent manner (Fig. 4A, white squares). The ratio of non-aggregated lysosomes decreased in the CPZ treated group, and the average size of individual lysosomes increased in the CPZ treated group (Fig. 4B). The percentage of non-aggregated lysosomes decreased gradually in the FXT treated group (Fig. 4C). The mean size of each non-aggregated lysosome increased up to 40 μM and then decreased at 80 μM. A decreased proportion of non-aggregated lysosomes along with an increased size of lysosomes were observed at up to 10 μM PXT treatment (Fig. 4D). This decreased proportion of area was restored, and size remained the same at 20 μM. No change in the proportion of non-aggregated lysosomes was observed compared to the total lysosomal area in the DOX and MET treatments (Fig. 4E and F). No difference in the average size of non-aggregated lysosomes was observed in either non-lysosomotropic compound treatment. Therefore, no effect on the distribution and size of lysosomes was detected by non-lysosomotropic compounds. These results indicate that the new parameters using distribution and size of lysosomes can be used to identify lysosomotropism of compounds.

4. Discussion

Lysosomal accumulation of drugs not only affects drug activity but also induces toxicity and side effects, e.g., phospholipidosis. Moreover, lysosomal accumulation of two or more drugs causes unpredictable drug interactions [16]. Therefore, it is important to understand whether a drug accumulates within lysosomes. In contrast, cancer cell-targeted therapies applying lysosomotropism have been attempted through induction of cell death using lysosomotropic compounds or nanoparticles that accumulate within lysosomes because lysosomotropic compounds induce the release of intralysosomal hydrolases into the cytoplasm by LMP, which leads to cancer cell death through necrosis or apoptosis [22]. Various high-throughput studies have been conducted to identify lysosomotropic compounds for these preventive or therapeutic purposes.

Because of improved image acquisition technology, it has become possible to obtain high-resolution images in a short time. Moreover, a large number of samples can be processed rapidly through automation. Furthermore, the development of image analysis technology makes it possible to extract a maximum amount of information from an image. Thus, the utility of image-based phenotypic screening has been increasing. Screening methods for identifying lysosomotropism have been developed and verified in several studies. However, the high data content from images was not fully utilized because earlier HCS was mainly based on a simple comparison of the number of cells and the area of lysosomes. However, the intracellular distribution of lysosomes can change depending on intracellular pH [14,15]. In addition, lysosomal volume increases through osmotic attraction of water to the lysosome by the accumulation of lysosomotropic compounds. Therefore, it is possible to observe a larger lysosomal fluorescence area with a two-dimensional image when lysosomotropic compounds are used [16]. In this study, the changes in the intracellular distribution of lysosomes and individual lysosomal size were used as markers to determine lysosomotropism of compounds by phenotypic screening using a newly developed image analysis method.

Four lysosomotropic compounds increased lysosomal area, whereas the area remained unchanged for two non-lysosomotropic compounds after using the conventional screening method. It was possible to identify lysosomotropic drugs using the new parameters that evaluate the size and distribution of the lysosomes through the degree of aggregation. The ratio of non-aggregated lysosomal area decreased compared with that in the control group following treatment with a lysosomotropic compound. This phenomenon was not observed in the non-lysosomotropic compound treated group. Furthermore, an increase in the size of individual lysosomes was observed in the lysosomotropic agent treated group. The interpretation was difficult with the conventional analytic method for such compounds that affect cell viability or induce lysosomal permeabilization (Supplementary Fig. 1D, 20 μM of PXT). However, the new parameters provided additional information that helped in interpreting lysosomotropism (Fig. 4D). The new parameters based on the distribution and size of the lysosomes were less affected by compound cytotoxicity than those of the conventional parameters because total cytoplasmic area was not used for normalization (Fig. 1). This result suggests that lysosomotropic compounds can be screened using one lysosome-specific fluorescent marker such as Lysotracker without staining the cytoplasm or nucleus. These new parameters will improve the reliability of the screening to identify lysosomotropic compounds.

Based on our experiments, lysosomes were susceptible to photodestruction. In addition, photosensitization of lysosomes by treatment with lysosomotropic agents has been reported [20,23]. It is better to use experimental settings that avoid photodestruction of the lysosome from lysosomal photosensitization by lysosomotropic fluorescence and repetitive laser exposure particularly for experiments that stain lysosomes with many other targets such as autophagosome simultaneously. Thus, it is necessary to adjust the exposure time and the intensity of the laser to obtain high resolution images without photodamage to lysosomes.

Various methods for identifying the lysosomal accumulation of drugs have been proposed; however, no standard method is available. We provided the convenience and accuracy of an image based screening method using new imaging technology. We introduced and confirmed two new parameters based on the distribution and the size of lysosomes for identifying lysosomotropism. These new parameters help identify lysosomotropism without interfering with the cytotoxicity of the test compound. The accuracy of the conventional analytic methods can be improved with these newly introduced analytic parameters. Increasing screening accuracy can help solve the problem of repetitive experiments to identify lysosomotropism of one drug with various concentrations.

Acknowledgment

This work was supported by the research promoting grant from the Keimyung University Dongsan Medical Center in 2006.

Appendix A. Supplementary data

Supplementary data associated with this article can be found, in the online version, at http://dx.doi.org/10.1016/j.bbrc.2014.05.091.

References

[1] C. de Duve, Lysosomes revisited, Eur. J. Biochem. 137 (1983) 391–397.
[2] S. Nadanaciva, S. Lu, D.F. Gebhard, et al., A high content screening assay for identifying lysosomotropic compounds, Toxicol. In Vitro 25 (2011) 715–723.
[3] S. Ohkuma, B. Poole, Fluorescence probe measurement of the intralysosomal pH in living cells and the perturbation of pH by various agents, Proc. Natl. Acad. Sci. U.S.A. 75 (1978) 3327–3331.
[4] M. Forgac, Vacuolar ATPases: rotary proton pumps in physiology and pathophysiology, Nat. Rev. Mol. Cell Biol. 8 (2007) 917–929.
[5] T. Aki, A. Nara, K. Uemura, Cytoplasmic vacuolization during exposure to drugs and other substances, Cell Biol. Toxicol. 28 (2012) 125–131.
[6] C. de Duve, A. Trouet, D.D. Campeneere, et al., Liposomes as lysosomotropic carriers, Ann. N. Y. Acad. Sci. 308 (1978) 226–234.
[7] B. Poole, S. Ohkuma, Effect of weak bases on the intralysosomal pH in mouse peritoneal macrophages, J. Cell Biol. 90 (1981) 665–669.
[8] R.L. Robison, G.E. Visscher, S.A. Roberts, et al., Generalized phospholipidosis induced by an amphiphilic cationic psychotropic drug, Toxicol. Pathol. 13 (1985) 335–348.
[9] F. Kazmi, T. Hensley, C. Pope, et al., Lysosomal sequestration (Trapping) of lipophilic amine (cationic amphiphilic) drugs in immortalized human hepatocytes (Fa2N-4 cells), Drug Metab. Dispos. 41 (2013) 897–905.
[10] F.M. van de Water, J. Havinga, W.T. Ravesloot, et al., High content screening analysis of phospholipidosis: validation of a 96-well assay with CHO-K1 and HepG2 cells for the prediction of in vivo based phospholipidosis, Toxicol. In Vitro 25 (2011) 1870–1882.
[11] J. Coleman, Y. Xiang, P. Pande, et al., A live-cell fluorescence microplate assay suitable for monitoring vacuolation arising from drug or toxic agent treatment, J. Biomol. Screen. 15 (2010) 398–405.
[12] B. Lemieux, M.D. Percival, J.P. Falgueyret, Quantitation of the lysosomotropic character of cationic amphiphilic drugs using the fluorescent basic amine Red DND-99, Anal. Biochem. 327 (2004) 247–251.
[13] S.S. Choi, J.S. Kim, L.G. Valerio Jr., et al., In silico modeling to predict drug-induced phospholipidosis, Toxicol. Appl. Pharmacol. 269 (2013) 195–204.
[14] V.I. Korolchuk, S. Saiki, M. Lichtenberg, et al., Lysosomal positioning coordinates cellular nutrient responses, Nat. Cell Biol. 13 (2011) 453–460.
[15] J. Heuser, Changes in lysosome shape and distribution correlated with changes in cytoplasmic pH, J. Cell Biol. 108 (1989) 855–864.
[16] R.S. Funk, J.P. Krise, Cationic amphiphilic drugs cause a marked expansion of apparent lysosomal volume: implications for an intracellular distribution-based drug interaction, Mol. Pharm. 9 (2012) 1384–1395.
[17] G.W. Zack, W.E. Rogers, S.A. Latt, Automatic measurement of sister chromatid exchange frequency, J. Histochem. Cytochem. 25 (1977) 741–753.
[18] T.W. Ridler, S. Calvard, Picture thresholding using an iterative selection method, IEEE Trans. Syst. Man Cybern. 8 (1978) 630–632.
[19] J.M. Prewitt, M.L. Mendelsohn, The analysis of cell images, Ann. N. Y. Acad. Sci. 128 (1966) 1035–1053.
[20] G.J. Zhang, J. Yao, The direct cause of photodamage-induced lysosomal destabilization, Biochim. Biophys. Acta 1326 (1997) 75–82.
[21] J.K. Jaiswal, M. Fix, T. Takano, et al., Resolving vesicle fusion from lysis to monitor calcium-triggered lysosomal exocytosis in astrocytes, Proc. Natl. Acad. Sci. U.S.A. 104 (2007) 14151–14156.
[22] R.A. Ndolo, Y. Luan, S. Duan, et al., Lysosomotropic properties of weakly basic anticancer agents promote cancer cell selectivity in vitro, PLoS One 7 (2012) e49366.
[23] G. Ouedraogo, P. Morliere, M. Bazin, et al., Lysosomes are sites of fluoroquinolone photosensitization in human skin fibroblasts: a microspectrofluorometric approach, Photochem. Photobiol. 70 (1999) 123–129.
[24] L. Zhou, G. Geraci, S. Hess, et al., Predicting phospholipidosis: a fluorescence non cell based in vitro assay for the determination of drug-phospholipid complex formation in early drug discovery, Anal. Chem. 83 (2011) 6980–6987.
[25] U.M. Hanumegowda, G. Wenke, A. Regueiro-Ren, et al., Phospholipidosis as a function of basicity, lipophilicity, and volume of distribution of compounds, Chem. Res. Toxicol. 23 (2010) 749–755.
[26] D.J. Pelletier, D. Gehlhaar, A. Tilloy-Ellul, et al., Evaluation of a published in silico model and construction of a novel Bayesian model for predicting phospholipidosis inducing potential, J. Chem. Inf. Model 47 (2007) 1196–1205.